IOPscience iopscience.iop.org

Home Search Collections Journals About Contact us My IOPscience

Angular distribution of positrons in coherent pair production in deformed crystals

This article has been downloaded from IOPscience. Please scroll down to see the full text article.

2009 J. Phys.: Condens. Matter 21 185401

(http://iopscience.iop.org/0953-8984/21/18/185401)

View the table of contents for this issue, or go to the journal homepage for more

Download details:
IP Address: 129.252.86.83
The article was downloaded on 29/05/2010 at 19:31

Please note that terms and conditions apply.

J. Phys.: Condens. Matter **21** (2009) 185401 (7pp) doi:10.1088/0953-8984/21/18/185401

Angular distribution of positrons in coherent pair production in deformed crystals

V V Parazian

Institute of Applied Problems in Physics, 25 Nersessian Street, 0014 Yerevan, Armenia

Received 21 November 2008, in final form 6 March 2009
Published 31 March 2009
Online at stacks.iop.org/JPhysCM/21/185401

Abstract

We investigate the angular distribution of positrons in the coherent process electron–positron pair creation process by high-energy photons in a periodically deformed single crystal with a complex base. The formula for the corresponding differential cross section is derived for an arbitrary deformation field. The case is considered in detail when the photon enters into the crystal at small angles with respect to a crystallographic axis. The results of the numerical calculations are presented for SiO_2 and diamond single crystals and Moliere parameterization of the screened atomic potentials in the case of the deformation field generated by an acoustic wave of S-type.

1. Introduction

The investigation of high-energy electromagnetic processes in crystals is of interest not only from the viewpoint of underlying physics but also from the viewpoint of practical applications. From the point of view of controlling the parameters of various processes in a medium, it is of interest to investigate the influence of external fields, such as acoustic waves, temperature gradient, etc, on the corresponding characteristics. The considerations of concrete processes, such as diffraction radiation [1], transition radiation [2], parametric x-radiation [3], channeling radiation [4] and bremsstrahlung by high-energy electrons [5], have shown that the external fields can essentially change the angular frequency characteristics of the radiation intensities. Recently there has been broad interest in compact crystalline undulators with periodically deformed crystallographic planes as an efficient source of high-energy photons [6] (for a review with a more complete list of references see [7]).

Motivated by the fact that the basic source for the creation of positrons for high-energy electron–positron colliders is the electron–positron pair creation by high-energy photons (for a recent discussion see, for example, [8]), in [9] we have investigated the influence of the hypersonic wave excited in a crystal on this process. To have an essential influence of the acoustic wave, high-frequency hypersound is needed. Usually this type of wave is excited by a high-frequency electromagnetic field through the piezoelectric effect in crystals with a complex base. In the papers [10, 11] we have generalized the results of [9] for crystals with a complex base and for acoustic waves with an arbitrary profile. For the experimental detection of final particles in the process of coherent pair production it is important to know their angular distribution. In the present paper the angular distribution of positrons in the coherent pair production in crystals is investigated in the presence of a hypersonic wave. The numerical calculations are carried out for quartz and diamond single crystals and for the photons of energies 20 and 100 GeV.

This paper is organized as follows. In section 2 we derive the general formula for the coherent part of the pair creation cross section averaged on thermal fluctuations and the conditions are specified under which the influence of the deformation field can be considerable. In section 3 the analysis of the general formula is presented in the cases when the photon enters into the crystal at small angles with respect to the crystallographic axes or planes and the results of the numerical calculations for the cross section as a function of the angle between the momenta of photon and positron are shown. Section 4 summarizes the main results of the paper.

2. Angular dependence of the cross section

By making use of the results for the bremsstrahlung derived in [12], after the redefinition of the variables, we find the differential cross section for the electron–positron pair

 © 2009 IOP Publishing Ltd Printed in the UK

production on an individual atom:

$$\frac{\mathrm{d}^5\sigma_{0\pm}}{\mathrm{d}\epsilon_+\,\mathrm{d}q_\parallel\,\mathrm{d}\mathbf{q}_\perp\,\mathrm{d}y} = \frac{e^2}{8\pi^4\omega^2}\frac{q_\perp^2}{q_\parallel^2} \times\left[\frac{\omega^2}{2\epsilon_+\epsilon_-} - 1 + 4y^2\frac{\delta_\pm}{q_\parallel}\left(1-\frac{\delta_\pm}{q_\parallel}\right)\right]\frac{|u(\mathbf{q})|^2}{\sqrt{1-y^2}} = |u(\mathbf{q})|^2\sigma_0(\mathbf{q},y), \tag{1}$$

where e is the electron charge, ω, ϵ_+ and ϵ_- are the energies of photon, positron and electron, respectively (the system of units $\hbar = c = 1$ is used), $\delta_\pm = m_\mathrm{e}^2\omega/(2\epsilon_+\epsilon_-)$, where m_e is the mass of electron, $q_\parallel$ and $q_\perp$ are the components of the vector of momentum transfer $\mathbf{q}$, $\mathbf{q} = \mathbf{k} - \mathbf{p}_+ - \mathbf{p}_-$ ($\mathbf{k}$, $\mathbf{p}_+$, $\mathbf{p}_-$ are the momenta of photon, positron and electron, respectively), parallel and perpendicular to the direction of the photon momentum, and $u(\mathbf{q})$ is the Fourier transform of the atom potential. The variable y is expressed in terms of the angle θ_+ between the momenta $\mathbf{k}$ and $\mathbf{p}_+$ by the following relation:

$$\left(\frac{\omega\theta_+}{m_\mathrm{e}}\right)^2 = \frac{1}{\delta_\pm}\left(q_\parallel - \delta_\pm - \frac{q_\perp^2}{2\omega} + \frac{q_\perp^2\delta_\pm}{m_\mathrm{e}^2}\right) + y\frac{2q_\perp}{m_\mathrm{e}}\left(\frac{q_\parallel}{\delta_\pm} - 1 - \frac{q_\perp^2}{2\omega\delta_\pm}\right)^{\frac{1}{2}}. \tag{2}$$

The regions of variables $q_\parallel$, $q_\perp$, y in cross section (1) are as follows [12]:

$$q_\parallel \geqslant \delta_\pm + \frac{q_\perp^2}{2\omega}, \qquad -1 \leqslant y \leqslant 1, \quad q_\perp \geqslant 0. \tag{3}$$

The differential cross section for the pair creation in a crystal can by written in the form [10]

$$\sigma(\mathbf{q},y) \equiv \frac{\mathrm{d}^5\sigma_{0\pm}}{\mathrm{d}\epsilon_+\,\mathrm{d}q_\parallel\,\mathrm{d}\mathbf{q}_\perp\,\mathrm{d}y} = \left|\sum_{n,j} u_\mathbf{q}^{(j)}\mathrm{e}^{\mathrm{i}\mathbf{q}\mathbf{r}_n^{(j)}}\right|^2\sigma_0(\mathbf{q},y), \tag{4}$$

where $\mathbf{r}_n^{(j)}$ is the position of an atom in the crystal. In the discussion that follows, the collective index n enumerates the elementary cell and the subscript j enumerates the atoms in a given cell of a crystal. Here $\mathbf{q}$ is the momentum transferred to the crystal, $\mathbf{q} = \mathbf{k} - \mathbf{p}_+ - \mathbf{p}_-$, and the differential cross section in a crystal given by (4) differs from the cross section on an isolated atom by the interference factor which is responsible for coherent effects arising due to the periodic arrangement of the atoms in the crystal. At non-zero temperature one has $\mathbf{r}_n^{(j)} = \mathbf{r}_{n0}^{(j)} + \mathbf{u}_{tn}^{(j)}$, where $\mathbf{u}_{tn}^{(j)}$ is the displacement of the jth atom with respect to the equilibrium positions $\mathbf{r}_{n0}^{(j)}$ due to the thermal vibrations. After averaging on thermal fluctuations, the cross section is written in the form (see, for instance [9] for the case of a crystal with a simple cell)

$$\sigma(\mathbf{q},y) = \left\{N\sum_j |u_\mathbf{q}^{(j)}|^2\left(1-\mathrm{e}^{-q^2\overline{u_t^{(j)2}}}\right) + \left|\sum_{n,j} u_\mathbf{q}^{(j)}\mathrm{e}^{\mathrm{i}\mathbf{q}\mathbf{r}_{n0}^{(j)}}\mathrm{e}^{-\frac{1}{2}q^2\overline{u_t^{(j)2}}}\right|^2\right\}\sigma_0(\mathbf{q},y), \tag{5}$$

where N is the number of cells, $\overline{u_t^{(j)2}}$ is the temperature-dependent mean-squared amplitude of the thermal vibrations of the jth atom and $\mathrm{e}^{-q^2\overline{u_t^{(j)2}}}$ is the corresponding Debye–Waller factor. In formula (5) the first term in braces does not depend on the direction of the vector $\mathbf{k}$ and determines the contribution of incoherent effects. The contribution of coherent effects is presented by the second term. By taking into account formula (1) for the cross section on a single atom, in the region $\omega q_\perp^2/\epsilon_+ m_\mathrm{e}^2 \ll 1$ the corresponding part of the cross section in a crystal can be presented in the form

$$\sigma_\mathrm{c} = \frac{e^2}{8\pi^4\omega^2}\frac{q_\perp^2}{q_\parallel^2}\left[\frac{\omega^2}{2\epsilon_+\epsilon_-} - 1 + 4y^2\frac{\delta_\pm}{q_\parallel}\left(1-\frac{\delta_\pm}{q_\parallel}\right)\right] \times\frac{1}{\sqrt{1-y^2}}\left|\sum_{n,j} u_\mathbf{q}^{(j)}\mathrm{e}^{\mathrm{i}\mathbf{q}\mathbf{r}_{n0}^{(j)}}\mathrm{e}^{-\frac{1}{2}q^2\overline{u_t^{(j)2}}}\right|^2. \tag{6}$$

When external influences are present (for example, in the form of acoustic waves) the positions of atoms in the crystal can be written as $\mathbf{r}_{n0}^{(j)} = \mathbf{r}_{ne}^{(j)} + \mathbf{u}_n^{(j)}$, where $\mathbf{r}_{ne}^{(j)}$ determines the equilibrium position of an atom in the situation without deformation and $\mathbf{u}_n^{(j)}$ is the displacement of the atom caused by the external influence. We consider deformations with the periodic structure

$$\mathbf{u}_n^{(j)} = \mathbf{u}_0 f(\mathbf{k}_s\mathbf{r}_{ne}^{(j)}), \tag{7}$$

where $\mathbf{u}_0$ and $\mathbf{k}_s$ are the amplitude and wavevector corresponding to the deformation field, $f(x)$ is an arbitrary function with the period 2π, $\max f(x) = 1$. In the discussion that follows, we assume that $f(x) \in C^\infty(R)$. Note that we can disregard the dependence of $\mathbf{u}_n^{(j)}$ on the time coordinate for the case of acoustic waves, as for the particle energies we are interested in, the characteristic time for the change of the deformation field is much greater compared with the passage time of particles through the crystal. For the deformation field given by equation (7) the sum over the atoms in equation (5) can be transformed into the form

$$\sum_n u_\mathbf{q}^{(j)}\mathrm{e}^{\mathrm{i}\mathbf{q}\mathbf{r}_{n0}^{(j)}} = \sum_{m=-\infty}^{\infty} F_m(\mathbf{q}\mathbf{u}_0)\sum_n u_\mathbf{q}^{(j)}\mathrm{e}^{\mathrm{i}\mathbf{q}_m\mathbf{r}_{ne}^{(j)}}, \tag{8}$$

where $\mathbf{q}_m = \mathbf{q} + m\mathbf{k}_s$ and $F_m(x)$ is the Fourier transform of the function $\mathrm{e}^{\mathrm{i}xf(t)}$:

$$F_m(x) = \frac{1}{2\pi}\int_{-\pi}^{\pi}\mathrm{e}^{\mathrm{i}xf(t)-\mathrm{i}mt}\,\mathrm{d}t. \tag{9}$$

Below we need to have the asymptotic behavior of this function for large values of m. For a fixed x and under the assumptions for the function $f(x)$ given above, by making use of the stationary phase method we can see that $F_m(x) \sim \mathrm{O}(|m|^{-\infty})$ for $m \longrightarrow \infty$.

For a lattice with a complex cell the coordinates of the atoms can be written as $\mathbf{r}_{ne} = \mathbf{R}_n + \boldsymbol{\rho}_j$, with $\mathbf{R}_n$ being the positions of the atoms for one of the primitive lattices and $\boldsymbol{\rho}_j$ are the equilibrium positions for other atoms inside the nth elementary cell with respect to $\mathbf{R}_n$. By taking this into account, one obtains

$$\sum_{m=-\infty}^{\infty} F_m(\mathbf{q}\mathbf{u}_0)\sum_{j,n} u_\mathbf{q}^{(j)}\mathrm{e}^{-\frac{1}{2}q^2\overline{u_t^{(j)2}}}\mathrm{e}^{\mathrm{i}\mathbf{q}_m\mathbf{r}_{ne}^{(j)}} = \sum_{m=-\infty}^{\infty} F_m(\mathbf{q}\mathbf{u}_0)S(\mathbf{q},\mathbf{q}_m)\sum_n \mathrm{e}^{\mathrm{i}\mathbf{q}_m\mathbf{R}_n}, \tag{10}$$

where

$$S(\mathbf{q},\mathbf{q}_m)=\sum_j u_{\mathbf{q}}^{(j)}\mathrm{e}^{\mathrm{i}\mathbf{q}_m\boldsymbol{\rho}^{(j)}}\mathrm{e}^{-\frac{1}{2}q^2\overline{u_t^{(j)2}}} \tag{11}$$

is the factor determined by the structure of the elementary cell. For thick crystals the sum over cells in (10) can be presented as a sum over the reciprocal lattice:

$$\sum_n \mathrm{e}^{\mathrm{i}\mathbf{q}_m\mathbf{R}_m}=\frac{(2\pi)^3}{\Delta}\sum_{\mathbf{g}}\delta(\mathbf{q}-\mathbf{g}_m),\qquad \mathbf{g}_m=\mathbf{g}-m\mathbf{k}_s, \tag{12}$$

where Δ is the unit cell volume and $\mathbf{g}$ is the reciprocal lattice vector. Due to the δ function in this formula, the corresponding momentum conservation is written in the form

$$\mathbf{k}=\mathbf{p}_+ +\mathbf{p}_- +\mathbf{g}-m\mathbf{k}_s, \tag{13}$$

where $-m\mathbf{k}_s$ stands for the momentum transfer to the external field. As the main contribution to the coherent part of the cross section comes from the longitudinal momentum transfer of order δ the influence of the external excitation may be considerable if $|m|k_s$ is of order δ. The corresponding condition will be specified later. Another consequence of the δ function in (12) is that the function (9) enters into the cross section in the form $F_m(\mathbf{g}_m\mathbf{u}_0)$. Now it can be seen that in the sum over m in (10) the main contribution comes from the terms for which $|m\mathbf{k}_s\mathbf{u}_0|\lesssim|\mathbf{g}\mathbf{u}_0|$, or equivalently $|m|\lesssim\lambda_s/a$, where $\lambda_s=2\pi/k_s$ is the wavelength of the external excitation and a is of the order of the lattice spacing. Indeed, for the terms with $|m\mathbf{k}_s\mathbf{u}_0|\gg|\mathbf{g}\mathbf{u}_0|$ one has $F_m(\mathbf{g}_m\mathbf{u}_0)\approx F_m(m\mathbf{k}_s\mathbf{u}_0)$ and the phase of the integrand in (9) is equal to $m[\mathbf{k}_s\mathbf{u}_0 f(t)-t]$. Under the condition $|\mathbf{k}_s\mathbf{u}_0 f'(t)|<1$ this phase has no stationary point and one has $F_m(m\mathbf{k}_s\mathbf{u}_0)=\mathrm{O}(|m|^{-\infty})$, $m\longrightarrow\infty$ and the corresponding contribution is strongly suppressed. By taking into account that, for practically important cases one has $\mathbf{k}_s\mathbf{u}_0\sim u_0/\lambda_s\ll 1$, we see that the assumption made means that the derivative $f'(t)$ is not too large. In a way similar to that used in [10], it can be seen that the square of the modulus for the sum (8) is written as

$$\left|\sum_{n,j}u_{\mathbf{q}}^{(j)}\mathrm{e}^{\mathrm{i}\mathbf{q}\mathbf{r}_{n0}^{(j)}}\mathrm{e}^{-\frac{1}{2}q^2\overline{u_t^{(j)2}}}\right|^2$$

$$=N\frac{(2\pi)^3}{\Delta}\sum_{m,\mathbf{g}}|F_m(\mathbf{g}_m\mathbf{u}_0)|^2|S(\mathbf{g}_m,\mathbf{g})|^2, \tag{14}$$

where N is the number of cells.

Substituting this expression into formula (6) and integrating over the vector $\mathbf{q}$ by using the δ function, for the cross section one obtains

$$\mathrm{d}\sigma=\int\sigma(\mathbf{q})\mathrm{d}^3q=N(\mathrm{d}\sigma_{\mathrm{n}}+\mathrm{d}\sigma_{\mathrm{c}}), \tag{15}$$

with $\mathrm{d}\sigma_{\mathrm{n}}$ and $\mathrm{d}\sigma_{\mathrm{c}}$ being the incoherent and coherent parts of the cross section per atom and N_0 is the number of atoms in the crystal. The coherent part of the cross section is determined by the formula

$$\frac{\mathrm{d}^2\sigma_{\pm}^{\mathrm{c}}}{\mathrm{d}\epsilon_+\,\mathrm{d}y}=\frac{e^2N}{\pi\omega^2N_0\Delta}\sum_{m,\mathbf{g}}\frac{g_{m\perp}^2}{g_{m\parallel}^2}\left[\frac{\omega^2}{2\epsilon_+\epsilon_-}-1+4y^2\frac{\delta_\pm}{g_{m\parallel}}\left(1-\frac{\delta_\pm}{g_{m\parallel}}\right)\right]\frac{|F_m(\mathbf{g}_m\mathbf{u}_0)|^2|S(\mathbf{g}_m,\mathbf{g})|^2}{\sqrt{1-y^2}}, \tag{16}$$

where the vector $\mathbf{g}_m$ is defined by relation (12) and now the relation between the variables y and θ_+ is written in the form

$$y=\frac{m_{\mathrm{e}}}{2g_{m\perp}}\times\frac{(\omega\theta_+/m_{\mathrm{e}})^2-1/\delta_\pm(g_{m\parallel}-\delta_\pm-g_{m\perp}^2/(2\omega)+g_{m\perp}^2\delta_\pm/m_{\mathrm{e}}^2)}{[g_{m\parallel}/\delta_\pm-1-g_{m\perp}^2/(2\omega\delta_\pm)]^{\frac{1}{2}}}. \tag{17}$$

The regions of variables in cross section (4) are

$$g_{m\parallel}\geqslant\delta_\pm+\frac{g_{m\perp}^2}{2\omega},\qquad -1\leqslant y\leqslant 1,\quad g_{m\perp}\geqslant 0. \tag{18}$$

For a sinusoidal deformation field, $f(z)=\sin(z+\varphi_0)$, one has the Fourier transform

$$F_m(x)=\mathrm{e}^{\mathrm{i}m\varphi_0}J_m(x), \tag{19}$$

with the Bessel function $J_m(x)$.

The formula for the pair creation in an undeformed crystal is obtained from (16) taking $\mathbf{u}_0=0$. In this limit, the contribution of the term with $m=0$ remains only with $F_0(0)=1$. Now we see that formula (16) differs from the formula in an undeformed crystal by the replacement $\mathbf{g}\to\mathbf{g}_m$ and by the additional summation over m with the weights $|F_m(\mathbf{g}_m\mathbf{u}_0)|^2$. This corresponds to the presence of an additional one-dimensional superlattice with the period λ_s and the reciprocal lattice vector $m\mathbf{k}_s$, $m=0,\pm1,\pm2,\ldots$. As the main contribution to the cross section comes from the terms with $g_{m\parallel}\sim\delta_\pm$, the influence of the deformation field may be considerable if $|mk_{s\parallel}|\gtrsim\delta_\pm$. Combining this with the previous estimates, we find the following condition: $u_0/\lambda_s\gtrsim a/4\pi^2l_c$. At high energies one has $a/l_c\ll 1$ and this condition can be consistent with the condition $u_0/\lambda_s\ll 1$.

In the presence of the deformation field the number of possibilities to satisfy the condition $g_{m\parallel}\geqslant\delta_\pm+g_{m\perp}^2/(2\omega)$ in the summation of formula (16) increases due to the term $mk_{s\parallel}$ in the expression for $g_{m\parallel}$. This leads to the appearance of additional peaks in the angular distribution of the radiated positrons. After the integration of (16) over y, due to these additional peaks, there can be an enhancement of the cross section of the process [10].

3. Limiting cases and numerical results

In the following, we consider the case when the photon enters into the crystal at small angle θ with respect to the crystallographic z axis of the orthogonal lattice. The corresponding reciprocal lattice vector components are $g_i=2\pi n_i/a_i$, $n_i=0,\pm1,\pm2,\ldots$, where a_i, $i=1,2,3$, are the lattice constants in the corresponding directions. For the longitudinal component we can write

$$g_{m\parallel}=g_{mz}\cos\theta+(g_{my}\cos\alpha+g_{mx}\sin\alpha)\sin\theta, \tag{20}$$

where α is the angle between the projection of the vector $\mathbf{k}$ on the plane (x,y) and axis y. For small angles θ the main contribution to the cross section comes from the summands

with $g_z = 0$. Having made the replacement of variable $y \to \omega\theta_+/m_e$ using formula (17) from formula (16) one finds

$$\frac{d^2\sigma^c_\pm}{d\epsilon_+ d(\omega\theta_+/m_e)} \approx \frac{e^2N}{\pi\omega^2N_0\Delta}\sum_{m,g_x,g_y}\frac{g_\perp^2}{g_{m\parallel}^2} \times\left[\frac{\omega^2}{2\epsilon_+\epsilon_-}-1+4y^2(\theta_+)\frac{\delta_\pm}{g_{m\parallel}}\left(1-\frac{\delta_\pm}{g_{m\parallel}}\right)\right] \times\frac{|F_m(\mathbf{g}_m\mathbf{u}_0)|^2|S(\mathbf{g}_m,\mathbf{g})|^2}{\sqrt{1-y^2(\theta_+)}} \times\frac{\omega\theta_+/m_e}{(g_\perp/m_e)(g_{m\parallel}/\delta_\pm-1-g_\perp^2/(2\omega\delta_\pm))^{\frac{1}{2}}}, \tag{21}$$

where the notation $y^2(\theta_+)$ is introduced in accordance with

$$y^2(\theta_+) = \frac{m_e^2}{4g_\perp^2}[(\omega\theta_+/m_e)^2-(1/\delta_\pm)(g_{m\parallel}-\delta_\pm-g_\perp^2/(2\omega) + g_\perp^2\delta_\pm/m_e^2)]^2[g_{m\parallel}/\delta_\pm-1-g_{m\perp}^2/(2\omega\delta_\pm)]^{-1}. \tag{22}$$

In (21) $g_\perp^2 = g_x^2+g_y^2$ and the summation goes over the region $g_{m\parallel} \geqslant \delta_\pm + g_{m\perp}^2/(2\omega)$, $0 \leqslant y^2(\theta_+) \leqslant 1$ with

$$g_{m\parallel} \approx -mk_z + (g_{mx}\sin\alpha + g_{my}\cos\alpha)\theta. \tag{23}$$

Note that in the argument of the functions F_m and S we have $\mathbf{g}_m \approx (g_x, g_y, 0)$.

We now assume that the photon enters into the crystal at a small angle θ with respect to the crystallographic axis z and near the crystallographic plane (y, z) (the angle α is small). In this case with the change of $\delta_\pm$, the sum over g_x and g_y will drop sets of terms which lead to the abrupt change of the corresponding cross section. Two cases have to be distinguished. Under the condition $\delta_\pm \sim 2\pi\theta/a_2$, in equation (21) for the longitudinal component, one has

$$g_{m\parallel} \approx -mk_{s\parallel} + \theta g_y \geqslant \delta_\pm + \frac{g_\perp^2}{2\omega}. \tag{24}$$

Formula (21) can be further simplified under the assumption $\mathbf{u}_0 \perp \mathbf{a}_1$. In this case, in the argument of the function F_m, one has $\mathbf{g}_m\mathbf{u}_0 \approx g_y u_{0y}$ and we obtain the formula

$$\frac{d^2\sigma^c_\pm}{d\epsilon_+ d(\omega\theta_+/m_e)} \approx \frac{e^2N}{\pi^2\omega^2N_0\Delta}\sum_{m,g_x,g_y}\frac{g_\perp^2}{g_{m\parallel}^2} \times\left[\frac{\omega^2}{2\epsilon_+\epsilon_-}-1+4y^2(\theta_+)\frac{\delta_\pm}{g_{m\parallel}}\left(1-\frac{\delta_\pm}{g_{m\parallel}}\right)\right] \times\frac{|F_m(g_y u_{y0})|^2|S(\mathbf{g}_m,\mathbf{g})|^2}{\sqrt{1-y^2(\theta_+)}} \times\frac{\omega\theta_+/m_e}{(g_\perp/m_e)[g_{m\parallel}/\delta_\pm-1-g_\perp^2/(2\omega\delta_\pm)]^{\frac{1}{2}}}. \tag{25}$$

In the second case, we assume that $\delta_\pm \sim 2\pi\theta\alpha/a_1$. Now the main contribution to the sum in equation (21) comes from terms with $g_y = 0$ and summations remain over m and n_1, $g_x = 2\pi n_1/a_1$. The formula for the cross section takes the form

$$\frac{d^2\sigma^c_\pm}{d\epsilon_+ d(\omega\theta_+/m_e)} \approx \frac{e^2N}{\pi^2\omega^2N_0\Delta}\sum_{m,n_1}\frac{g_{m\perp}^2}{g_{m\parallel}^2} \times\left[\frac{\omega^2}{2\epsilon_+\epsilon_-}-1+4y^2(\theta_+)\frac{\delta_\pm}{g_{m\parallel}}\left(1-\frac{\delta_\pm}{g_{m\parallel}}\right)\right] \times\frac{|F_m(\mathbf{g}_m\mathbf{u}_0)|^2|S(\mathbf{g}_m,\mathbf{g})|^2}{\sqrt{1-y^2(\theta_+)}} \times\frac{\omega\theta_+/m_e}{(g_{m\perp}/m_e)[g_{m\parallel}/\delta_\pm-1-g_{m\perp}^2/(2\omega\delta_\pm)]^{\frac{1}{2}}}, \tag{26}$$

where

$$g_{m\parallel} \approx -mk_z + g_x\psi, \qquad \psi = \alpha\theta, \tag{27}$$

and the summation goes over the values m and n_1 satisfying the condition $g_{m\parallel} \geqslant \delta_\pm + g_x^2/(2\omega)$.

We have carried out numerical calculations for the pair creation cross section for various values of parameters in the case of the SiO_2 single crystal at zero temperature. To deal with an orthogonal lattice, we choose as an elementary cell the cell including 6 atoms of silicon and 12 atoms of oxygen (the Shrauf elementary cell [13]). For this choice the y and z axes of the orthogonal coordinate system (x, y, z) coincide with the standard Y and Z axes of the quartz crystal, whereas the angle between the axes x and X is equal to $\pi/6$. For the potentials of atoms we take Moliere parameterization with

$$u_{\mathbf{q}}^{(j)} = \sum_{i=1}^{3}\frac{4\pi Z_j e^2\alpha_i}{q^2+(\chi_i/R_j)^2} \tag{28}$$

where $\alpha_i = \{0.1, 0.55, 0.35\}$, $\chi_i = \{6.0, 1.2, 0.3\}$ and R_j is the screening radius for the jth atom in the elementary cell.

The calculations are carried out for the sinusoidal transversal acoustic wave of S-type (the corresponding parameters can be found in [14]) for which the vector of the amplitude of the displacement is directed along the X direction of the quartz single crystal, $\mathbf{u}_0 = (u_0, 0, 0)$, and the velocity is 4.687×10^5 cm s^{-1}. The vector determining the direction of the hypersound propagation lies in the plane YZ and has an angle with the axis Z equal to 0.295 rad. As the axis z we choose the axis Z of the quartz crystal. The corresponding function $F(x)$ is determined by formula (9). In order to illustrate the dependence of the results on the type of crystal we also present the numerical data for the diamond monocrystal.

Numerical calculation shows that, in dependence of the values for parameters, the external excitation can either enhance or reduce the cross section of the pair creation process. As an illustration of the enhancement in the cross section integrated over the angle θ_+, in the left panel of figure 1 we have plotted the quantity $10^{-3}(m_e^2\omega/e^6)\,d\sigma^c_\pm/d\epsilon_+$, evaluated by using the formula from [10], as a function of the ratio ϵ_+/ω in the case of the SiO_2 monocrystal and Moliere parameterization of the screened atomic potential for $2\pi u_0/a_1 = 0$ (dashed curve) and $2\pi u_0/a_1 = 6.07$ (full curve). In the right panel the same quantity is plotted as a function of $2\pi u_0/a_1$ for the positron energy corresponding to $\epsilon_+/\omega = 0.5$. The values for the other parameters are taken as follows: $\omega = 20$ GeV, $\psi = 0.005\,52$, $\nu_s = 5\times10^9$ Hz

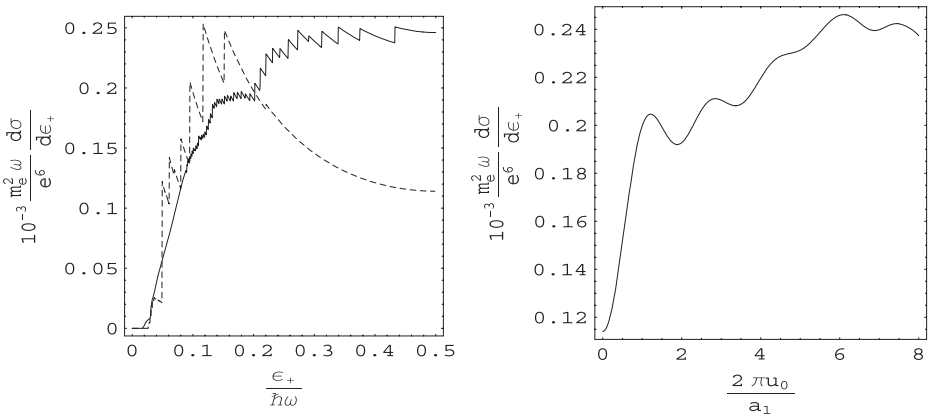

Figure 1. Coherent pair creation cross section, $10^{-3}(m_e^2\omega/e^6)\,d\sigma_\pm^c/d\epsilon_+$, evaluated by the formula from [10], as a function of ϵ_+/ω for $2\pi u_0/a_1 = 0$ (dashed curve), $2\pi u_0/a_1 = 6.07$ (full curve), and as a function of $2\pi u_0/a_1$ (right panel) for the positron energy corresponding to $\epsilon_+/\omega = 0.5$. The values for the other parameters are as follows: $\psi = 0.005\,52$, $\omega = 20$ GeV, $\nu_s = 5 \times 10^9$ Hz.

for the frequency of acoustic waves. For the amplitude of the deformation field corresponding to the numerical data of figure 1 the relative displacement of the neighboring atoms is of the order 10^{-3} Å, which is much smaller than the interatomic distance (∼5 Å).

For these values of parameters, when one has an enhancement of the cross section integrated over the angle θ_+, we have numerically analyzed the angular dependence of the pair creation cross section by making use of formula (26). In figure 2 the quantity $10^{-3}(m_e^2\omega/e^2)\,d^2\sigma_\pm^c/d\epsilon_+\,d\theta_+$ is depicted as a function of $\omega\theta_+/m_e$ in the case of the SiO_2 monocrystal for $u_0 = 0$ (dashed curve) and $2\pi u_0/a_1 = 6.07$ (full curve). The values for the other parameters are taken as follows: $\epsilon_+/\omega = 0.5$, $\omega = 20$ GeV, $\nu_s = 5 \times 10^9$ Hz, $\psi = 0.005\,52$.

In order to see the dependence of the results on the energy of the incoming photon, in figure 3 we have presented the quantity $10^{-3}(m_e^2\omega/e^2)\,d^2\sigma_\pm^c/d\epsilon_+\,d\theta_+$ as a function of $\omega\theta_+/m_e$ in the case of the SiO_2 monocrystal for the values of parameters ϵ_+, ψ and u_0 taken from [10], for which the integrated cross section is enhanced (reduced) by the acoustic wave. The dashed curves in both panels correspond to the situation when the deformation field is absent ($u_0 = 0$). The full curve in the left (right) panel is for the amplitude of the deformation field corresponding to the value $2\pi u_0/a_1 = 1.1$ (left panel, enhanced) ($2\pi u_0/a_1 = 2.14$, right panel, reduced). The values for the other parameters are as follows: $\epsilon_+/\omega = 0.5$, $\omega = 100$ GeV, $\nu_s = 5 \times 10^9$ Hz, $\psi = 0.001$.

It is also interesting to see the dependence of the results presented before on the type of crystal. In figure 4 we have plotted the quantity $10^{-6}(m_e^2\omega/e^2)\,d^2\sigma_\pm^c/d\epsilon_+\,d\theta_+$ as a function of $\omega\theta_+/m_e$ in the case of the diamond monocrystal for $u_0 = 0$ (dashed curves), $2\pi u_0/a_1 = 2.5$ (left panel, full curve, enhanced) and for $2\pi u_0/a_1 = 3.8$ (right panel, full curve, reduced). The values for the other parameters are taken as follows: $\epsilon_+/\omega = 0.5$, $\omega = 100$ GeV, $\nu_s = 5 \times 10^9$ Hz, $\psi = 0.001\,42$.

As we see from the presented examples, the presence of the deformation field leads to the appearance of additional peaks in the angular distribution of the emitted positron (or electron) even for such ranges of values of an angle of positron

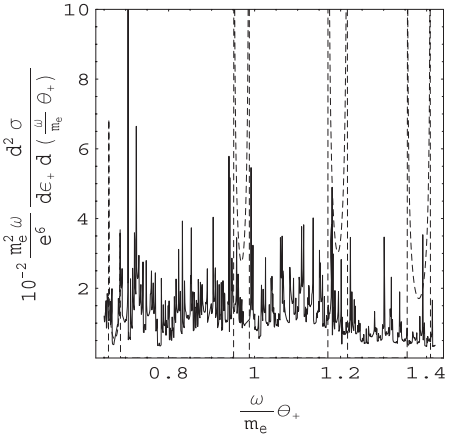

Figure 2. Coherent pair creation cross section, $10^{-3}(m_e^2\omega/e^6)d^2\sigma_\pm^c/d\epsilon_+\,d(\omega\theta_+/m_e)$, evaluated by formula (26), as a function of $\omega\theta_+/m_e$ for $2\pi u_0/a_1 = 0$ (dashed curve), $2\pi u_0/a_1 = 6.07$ (full curve) and $\psi = 0.005\,52$. The values for the other parameters are as follows: $\epsilon_+/\omega = 0.5$, $\omega = 20$ GeV, $\nu_s = 5 \times 10^9$ Hz for the frequency of acoustic waves.

momentum, where, due to the requirement $-1 \leqslant y \leqslant 1$, the cross section of the process is zero when the deformation is absent. As we have already mentioned before, this is related to that, in the presence of the deformation field, the number of possibilities to satisfy the condition $g_{m\parallel} \geqslant \delta_\pm + g_{m\perp}^2/(2\omega)$ in the summation in formula (16) increases due to the presence of the additional term $mk_{s\parallel}$ in the expression for $g_{m\parallel}$.

4. Conclusion

The present paper is devoted to the investigation of the angular distribution of the positron in the pair creation process by high-energy photons in a crystal with a complex lattice base in the presence of a deformation field of an arbitrary periodic profile. The latter can be induced, for example, by acoustic waves. The influence of the deformation field can serve as a possible mechanism to control the angular-energetic characteristics of the created particles. The importance of this is motivated by the

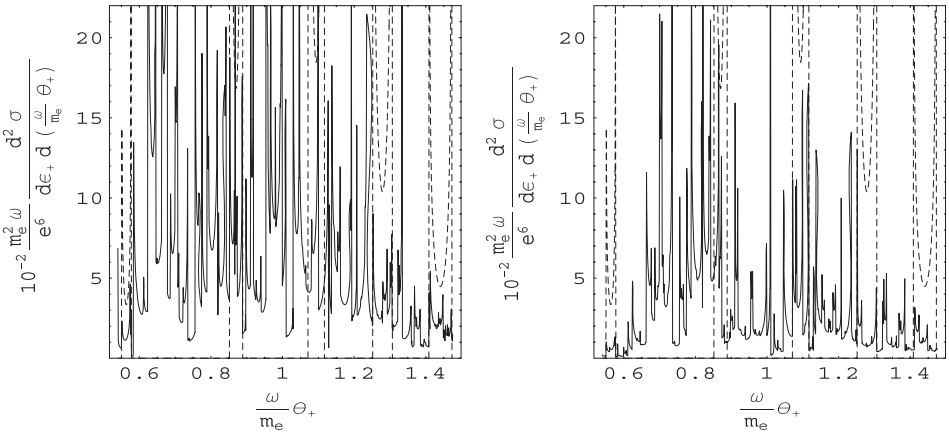

Figure 3. Coherent pair creation cross section for the SiO_2 crystal, $10^{-3}(m_e^2\omega/e^6)\,d^2\sigma_\pm^c/d\epsilon_+\,d(\omega\theta_+/m_e)$, evaluated by formula (26), as a function of $\omega\theta_+/m_e$ for $2\pi u_0/a_1 = 0$ (dashed curve), $2\pi u_0/a_1 = 1.1$ (full curve) and $\psi = 0.001$ (left panel) and as a function of $\omega\theta_+/m_e$ for $2\pi u_0/a_1 = 0$ (dashed curve), $2\pi u_0/a_1 = 2.14$ (full curve) and $\psi = 0.001$ (right panel). The values for the other parameters are as follows: $\epsilon_+/\omega = 0.5$, $\omega = 100$ GeV, $\nu_s = 5 \times 10^9$ Hz for the frequency of acoustic waves.

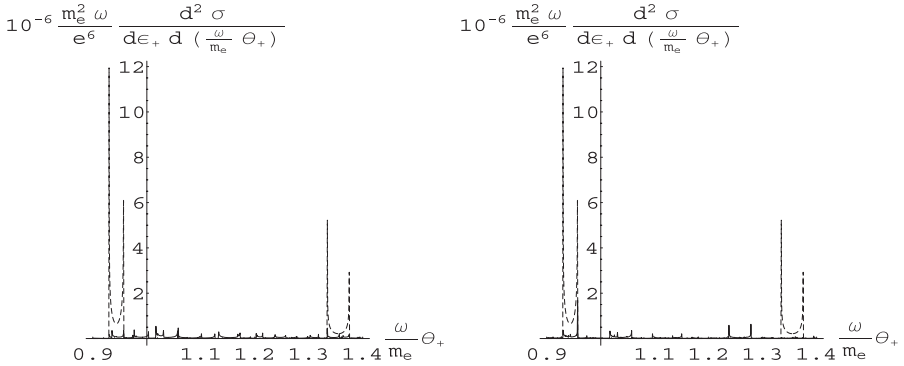

Figure 4. Coherent pair creation cross section for the diamond crystal, $10^{-6}(m_e^2\omega/e^6)\,d^2\sigma_\pm^c/d\epsilon_+\,d(\omega\theta_+/m_e)$, evaluated by formula (26), as a function of $\omega\theta_+/m_e$ for $2\pi u_0/a_1 = 0$ (dashed curve), $2\pi u_0/a_1 = 2.5$ (full curve) and $\psi = 0.001\,42$ (left panel) and as a function of $\omega\theta_+/m_e$ for $2\pi u_0/a_1 = 0$ (dashed curve), $2\pi u_0/a_1 = 3.8$ (full curve) and $\psi = 0.001\,42$ (right panel). The values for the other parameters are as follows: $\epsilon_+/\omega = 0.5$, $\omega = 100$ GeV, $\nu_s = 5 \times 10^9$ Hz for the frequency of acoustic waves.

fact that the basic source for creating positrons for high-energy colliders is the electron–positron pair creation by high-energy photons. In a crystal the cross section is a sum of coherent and incoherent parts. The coherent part of the cross section per single atom, averaged over thermal fluctuations, is given by formula (16). In this formula the factor $|F_m(\mathbf{g}_m\mathbf{u}_0)|^2$ is determined by the function describing the displacement of the atoms due to the deformation field and the factor $|S(\mathbf{g}_m, \mathbf{g})|^2$ is determined by the structure of the crystal elementary cell. Compared with the cross section in an undeformed crystal, formula (17) contains an additional summation over the reciprocal lattice vector of the one-dimensional superlattice induced by the deformation field. We have argued that the influence of the deformation field on the cross section can be remarkable under the condition $4\pi^2 u_0/a \gtrsim \lambda_s/l_c$. Note that, for the deformation with $4\pi^2 u_0/a > 1$, this condition is less restrictive than the naively expected one $\lambda_s \leqslant l_c$. The role of coherence effects in the pair creation cross section is essential when the photon enters into the crystal at small angles with respect to a crystallographic axis. In this case the main contribution to the coherent part of the cross section comes from the crystallographic planes, parallel to the chosen axis (z axis in our consideration). The behavior of this cross section as a function of the positron energy essentially depends on the angle θ between the projection of the photon momentum on the plane (x, y) and the y axis. When the photon enters into the crystal near a crystallographic plane, two cases have to be distinguished. For the first one ($\theta \sim a_2/2\pi l_c$) formula (21) is further simplified to the form (25) under the assumption $\mathbf{u}_0 \perp \mathbf{a}_1$. In the second case one has $\psi = \alpha\theta \sim a_1/2\pi l_c$ and the main contribution to the cross section comes from the crystallographic planes parallel to the incidence plane. The corresponding formula for the cross section takes the form (26). The numerical calculations for the cross section are carried out in the case of the SiO_2 single crystal with the Moliere parameterization of the screened atomic potentials and for the deformation field generated by the transversal acoustic wave of S-type with frequency 5 GHz. In order to illustrate the dependence of the results on the type of crystal we have also presented the results for the diamond monocrystal. Examples of numerical results are presented in the figures. The numerical calculations for values of the parameters in the problem when

one has an enhancement of the cross section show that the presence of the deformation field leads to the appearance of additional peaks in the angular distribution of the radiated positron (or electron) even for such ranges of values of an angle of a positron where, due to the requirement $-1 \leqslant y \leqslant 1$, the cross section is zero when the deformation is absent. This can be used to control the parameters of the positron sources for storage rings and colliders.

Acknowledgment

I am grateful to Aram Saharian for valuable discussions and suggestions.

References

[1] Mkrtchyan A R, Grigoryan L Sh, Didenko A N, Saharian A A and Mkrtchyan A G 1989 *Izv. Akad. Nauk Arm. SSR Fiz.* **24** 62
Mkrtchyan A R, Grigoryan L Sh, Didenko A N and Saharian A A 1991 *Sov. Phys.—JETP* **61** 21
Mkrtchyan A R, Grigoryan L Sh, Saharian A A and Didenko A N 1991 *Acustica* **75** 1984
Saharian A A, Mkrtchyan A R, Gevorgian L V, Grigoryan L Sh and Khachatryan B V 2001 *Nucl. Instrum. Methods* B **173** 211

[2] Grigoryan L Sh, Mkrtchyan A H and Saharian A A 1998 *Nucl. Instrum. Methods* B **145** 197

[3] Mkrtchyan A R, Aslanyan H A, Mkrtchyan A H and Gasparyan R A 1991 *Phys. Lett.* A **152** 297

[4] Mkrtchyan A R, Gasparyan R A and Gabrielyan R G 1986 *Phys. Lett.* A **115** 410
Mkrtchyan A R, Gasparyan R A and Gabrielyan R G 1987 *JETP* **93** 432
Mkrtchyan A R, Gasparyan R A and Gabrielyan R G 1988 *Phys. Lett.* A **126** 528
Grigoryan L Sh *et al* 2000 *Radiat. Eff. Defects Solids* **152** 13
Grigoryan L Sh *et al* 2000 *Radiat. Eff. Defects Solids* **152** 225
Grigoryan L Sh *et al* 2000 *Radiat. Eff. Defects Solids* **152** 269
Grigoryan L Sh *et al* 2001 *Radiat. Eff. Defects Solids* **153** 221
Grigoryan L Sh *et al* 2001 *Radiat. Eff. Defects Solids* **153** 289
Grigoryan L Sh *et al* 2001 *Radiat. Eff. Defects Solids* **153** 307
Grigoryan L Sh *et al* 2001 *Nucl. Instrum. Methods* B **173** 13
Grigoryan L Sh *et al* 2001 *Nucl. Instrum. Methods* B **173** 184
Grigoryan L Sh, Mkrtchyan A H, Khachatryan H F, Tonoyan V U and Wagner W 2003 *Nucl. Instrum. Methods* B **201** 25

[5] Saharian A A, Mkrtchyan A R, Parazian V V and Grigoryan L Sh 2004 *Mod. Phys. Lett.* A **19** 99
Parazian V V 2006 *J. Contemp. Phys.* **41** 221
Mkrtchyan A R, Saharian A A and Parazian V V 2008 arXiv:0810.0615

[6] Korol A V, Solov'yov A V and Greiner W 1998 *J. Phys. G: Nucl. Part. Phys.* **24** L45
Korol A V, Solov'yov A V and Greiner W 1999 *Int. J. Mod. Phys.* E **8** 49
Avakian R O, Gevorgian L A, Ispirian K A and Ispirian R K 1998 *JETP Lett.* **68** 467
Zhang Q-R 1999 *Int. J. Mod. Phys.* E **8** 493
Mikkelsen U and Uggerhøj E 2000 *Nucl. Instrum. Methods* B **160** 435
Korol A V, Solov'yov A V and Greiner W 2001 *J. Phys. G: Nucl. Part. Phys.* **27** 95
Avakian R O, Gevorgian L A, Ispirian K A and Ispirian R K 2001 *Nucl. Instrum. Methods* B **173** 112
Korol A V, Krause W, Solov'yov A V and Greiner W 2002 *Nucl. Instrum. Methods* A **483** 455
Avakian R O, Avetyan K T, Ispirian K A and Melikyan E G 2003 *Nucl. Instrum. Methods* A **508** 496
Bellucci S *et al* 2003 *Phys. Rev. Lett.* **90** 034801
Bellucci S 2005 *Mod. Phys. Lett.* B **19** 85
Bellucci S and Maisheev V A 2006 *Nucl. Instrum. Methods* B **252** 339

[7] Korol A V, Solov'yov A V and Greiner W 2004 *Int. J. Mod. Phys.* E **13** 867

[8] Artru X *et al* 2008 *Nucl. Instrum. Methods* B **266** 3868

[9] Mkrtchyan A R, Saharian A A, Grigoryan L Sh and Khachatryan B V 2002 *Mod. Phys. Lett.* A **17** 2571

[10] Mkrtchyan A R, Saharian A A and Parazian V V 2006 *Mod. Phys. Lett.* B **20** 1617

[11] Mkrtchyan A R, Saharian A A, Parazian V V, Mkrtchyan A H, Vardapetyan H A, Sirunyan A M, Hakobyan G G and Manukyan J V 2006 *J. Contemp. Phys.* **41** 29

[12] Akhiezer A I, Boldyshev V F and Shulga N F 1975 *J. Nucl. Phys.* **22** 1185

[13] Dana J S, Dana E S and Frondel C 1962 *The System of Mineralogy* (*Silica Minerals*) vol 3 (New York: Wiley)

[14] Shaskolskaya M P (ed) 1982 *Acoustic Crystals* (Moscow: Nauka) (in Russian)